Research Repository UCD

Provided by the author(s) and University College Dublin Library in accordance with publisher policies. Please cite the published version when available.

Title	Block copolymer mediated stabilization of sub-5 nm superparamagnetic nickel nanoparticles in an aqueous medium
Authors(s)	Bala, Tanushree; Gunning, Robert Denis; Venkatesan, Munuswamy; Godsell, Jeffrey F.; Roy, Saibal; Ryan, Kevin M.
Publication date	2009-10-14
Publication information	Nanotechnology, 20 (41): 415603
Publisher	IOP Science
Link to online version	http://dx.doi.org/10.1088/0957-4484/20/41/415603
Item record/more information	http://hdl.handle.net/10197/2715
Publisher's version (DOI)	10.1088/0957-4484/20/41/415603

Downloaded 2022-03-05T04:16:27Z

The UCD community has made this article openly available. Please share how this access benefits you. Your story matters! (@ucd_oa)

© Some rights reserved. For more information, please see the item record link above.

Block copolymer mediated stabilization of sub-5 nm superparamagnetic nickel nanoparticles in an aqueous medium

Tanushree Bala,[1] Robert Denis Gunning,[2] Munuswamy Venkatesan,[3] Jeffrey F. Godsell,[4] Saibal Roy[4] and Kevin M. Ryan[1, 2*]

[1] Materials and Surface Science Institute and Department of Chemical and Environmental Sciences, University of Limerick, Limerick, Ireland
[2] SFI-Strategic Research Cluster in Solar Energy Research, University of Limerick, Limerick, Ireland.
[3] School of Physics, Trinity College Dublin, Dublin-2, Ireland.
[4] Microsystems Centre, Tyndall National Institute, University College Cork, Cork, Ireland.

*To whom correspondence should be addressed: E-mail: kevin.m.ryan@ul.ie

Abstract
The paper presents a facile method for decreasing the size of water dispersible Ni nanoparticles from 30 nm to 3 nm by the incorporation of a passivating surfactant combination of pluronic triblock copolymer and oleic acid into a wet chemical reduction synthesis. A detailed study revealed that the size of the Ni nanoparticles is critically governed not only by the concentration of the tri block copolymers but also dependent on the hydrophobic nature of the micelle-core formed. The synthesized Ni nanoparticles were thoroughly characterized by TEM, XRD, XPS and temperature and field dependent magnetic measurements along with a comprehensive FTIR analysis to predict a possible mechanism of formation.

1. Introduction.

Magnetic nanoparticles have been successfully incorporated into data storage devices [1], ferro-fluides [2], magnetic resonance imaging (MRI) techniques [3], hyperthermia treatments [4] and targeted drug delivery [5]. Continued development of such applications for electronics, catalytic and medical diagnostics industries [6-8] requires synthetic protocols that can tune the size of the particles to the sub 5 nm range in high yield. Of the magnetic nanoparticles prepared from transition metals and their oxides[9], Ni nanoparticles have drawn additional interest as one of the most important catalysts for various reactions such as decomposition of ammonia [10], oxidative dehydrogenation [11], steam reforming [12], hydrogenation [13] and more recently the formation of carbon nanotubes (CNTs) [14]. Extensive applications of Ni based nanoparticles in biological systems are also reported. For example, Mirkin and co-workers demonstrated the efficient and selective separation of His-tagged proteins using Ni-based nanorods with a diameter of about 300 nm [15]. Hyeon and co-workers have successfully proved that superparamagnetic Ni with NiO shells have a high affinity for poly histidine and can be utilized for separating and purifying His-tagged proteins from a multicomponent solution [16].

Ni nanoparticles can be synthesised in both organic and aqueous media. The high temperature decomposition of nickel carbonyl compounds [17] or $Ni(acac)_2$ compounds [18] in the presence of oleylamine, tri octyl phosphine oxide (TOPO) and tri octyl phosphine (TOP) [19] are common organic routes. While these methods are capable of producing monodispersed Ni with sub 5 nm size range, partial oxidation on the surface of the particles occurs readily even with the use of more than one capping agent [19]. Furthermore, the complexity involved in the above synthetic procedures is quite evident, requiring many steps, higher temperature, inert atmosphere and the use of non-regular, toxic chemicals. Microemulsion based methods using mixtures of polar and non polar solvents have also

been successful, with sub 30 nm particle sizes reported, although the dependence of particle size on colloidal droplet size has limited the formation of sub 5 nm particles in high yield [20-22]. Recently, Prasad and co-workers have reported an interesting alternative avenue for the synthesis of Co and Ni nanoparticles in water using simple salts routinely available in the laboratory as metal sources with an option for scaling up the yield relatively easily [23]. The size of the Ni nanoparticles achieved by this route is quite large (≥30 nm) and many of the earlier reports found a particle of this size range as ferromagnetic like bulk Ni, not superparamagnetic [24,25]. This may limit applications, as the smaller superparamagnetic particles are crucial for diverse biological applications [26-28] allowing for ease of elimination when intravenously administered [29]. Also, as Ni nanoparticles are widely used for the growth of CNTs, smaller particles with narrow size distribution are more attractive for single walled CNT growth [30,31] or for other catalytic reactions[32]. The control over the particle size in nanoparticle synthesis depends on the stabilizing ability of the capping ligands [9]. Pluronic tri block co-polymers have recently shown promise as capping agents for particle size control in noble metals [33-37] and magnetic oxide nanoparticles [38-39] but have not been used for the synthesis of elemental magnetic nanoparticles.

Herein we report the dimensionally controlled synthesis of Ni nanoparticles in an aqueous solution using Pluronic tri block co-polymers which consist of poly ethylene oxide (PEO) and poly propylene oxide (PPO) in the general formula $(PEO)_x(PPO)_y(PEO)_x$. These amphiphiles can self assemble in aqueous solution to form micelles with their PPO chains as a hydrophobic core and the PEO open ends as hydrophilic corona. In this study the overall concentration was kept in the range where the possibility of forming higher lyophobic liquid crystalline (LLC) structure can be ruled out [40]. The study was aimed to reduce the size of the Ni particles and it was found that the colloidal stability of Ni nanoparticles proved to be related to the amphiphilic character of the tri block copolymer micelles at ambient temperature. The strategy has the distinct advantage of controlling the growth of the Ni particles in the hydrophobic micellar core which is enveloped with hydrophilic PEO corona of the polymer making it thoroughly water dispersible. As metallic magnetic nanoparticles can be toxic for biological systems, the surface passivation of Ni particles with bio-compatible block copolymers may allow for the realisation of bio-medical applications.

2. Experimental Details.

2.1. Materials.

Nickel nitrate hexahydrate ($Ni(NO_3)_2 \cdot 6H_2O$), sodium dodecyl sulfate (SDS), oleic acid (9-octadecenoic acid, mentioned as OA in text and figure captions) and sodium borohydride ($NaBH_4$) were purchased from Sigma Aldrich and used as-received. Pluronic block co-polymer (PEO-PPO-PEO) namely P123, P65, P85, F127 and F88 were supplied by BASF, Table 1 shows properties of the co-polymers used in this study.

2.2 Preparation and purification of Nickel Nanoparticles.

In a typical experiment (Reaction R_1), an aqueous mixture of $1X10^{-3}$ M $Ni(NO_3)_2 \cdot 6H_2O$ was taken with $1X10^{-2}$ M SDS and $1X10^{-4}$ M oleic acid and reduced with 0.035 g of solid $NaBH_4$, the exact details of this synthesis is described elsewhere [23]. We used methanolic solution of OA as it is not directly soluble in water. To the solution containing SDS and OA, various amount of Pluronic P123 were added to keep the concentration as 0.15% (Reaction R_2), 0.3% (Reaction R_3) and 3% (Reaction R_4). In another set of experiments $1X10^{-3}$ M $Ni(NO_3)_2 \cdot 6H_2O$ and $1X10^{-4}$ M OA were mixed with 3% (Reaction R_5) and 5% (Reaction R_6) of Pluronic P123. Note that we did not add SDS in R_5 and R_6. The solution was then reduced with 0.035 g of solid $NaBH_4$ and the colour of the solution turned black almost immediately after the addition of the reducing agent indicating the reduction of the Ni^{2+} to Ni^0. The solutions were kept at ambient conditions for 30 min to ensure the completion of the reaction. The solutions were then subjected to repeated centrifugation at 8000 rpm for 15 min followed by the separation of the supernatant and pellet. The pellet thus obtained was washed by a copious amount of

de-ionized water and re-centrifuged under the same conditions. The pellet received after the second centrifugation could be dispersed in water and the solution was used for characterizations. The centrifuged pellet was heated under N_2 atmosphere at 250 ^oC for ~30 min for XRD, FTIR and XPS characterizations.

We have also used other tri block copolymers in place of P123 namely 3% P65, 3% P85, 3% F127, 3% F88, a mixture of 3% P65/P123 and a mixture of 3% F127/P123 for synthesis of Ni nanoparticles. Here also, OA was added maintaining the same concentration of 10^{-4} M without any SDS.

2.3. Characterizations techniques.

2.3.1. Transmission electron microscopy. Samples for TEM were prepared by putting a drop of the nickel nanoparticle solution on a carbon-coated copper grid allowing to dry. TEM analysis was performed on a JEOL 2011 TEM instrument operated at an accelerating voltage of 200 KV.

2.3.2. X-ray diffraction analysis. X-ray diffractograms of the air dried samples and the heated samples were carried out an a PANalytical X'Pert MPD Pro using Cu K_α radiation with a 1-D X'Celerator strip detector.

2.3.3. Fourier transform infrared spectroscopy. FTIR measurements for the heated Ni samples were carried out on a Perkin-Elmer-Spectrum One FTIR spectrometer operated at a resolution of 4 cm^{-1}. The FTIR spectra of pure P123, OA and SDS were also measured for comparison.

2.3.4. X-ray photoelectron spectroscopy. XPS measurement of the heated Ni nanoparticles was carried out using a Kratos Axis 165 spectrometer. The general scan of C 1s, O 1s, Ni 2p, S 2p, were carried out with monochromated Al Kα with an energy of photoexcitation of 1486.58 eV. The overall resolution was 1 eV for the XPS measurements. The core level spectra were background corrected using the Shirley algorithm and the chemically distinct species were resolved using a nonlinear least squares fitting procedure. The core level binding energies (BE) were aligned with the adventitious carbon binding energy of 284.8 eV. The pass energy was 160 eV for a survey spectra and 20 eV for the narrow scans.

2.3.5. Magnetic Measurements. Magnetic measurements were performed on a Quantum Design MPMS XL5 SQUID magnetometer. For the field-cooled measurement, a magnetic field of 1 mT was applied, while for the M-H sweeps, fields of -5 T to +5 T were applied.

3. Results and discussion.

Ni nanoparticles of approximately 34 nm in size could be routinely synthesized by a wet chemical method using SDS and OA as surfactants with optimum concentration of 10^{-2} M and 10^{-4} M respectively [23]. This reaction (R_1) is perfectly reproducible and the as-synthesized particles are monodisperse and crystalline (fcc Ni). The basic characterizations of these particles are presented in Supporting information, S1. In this work, we found that the addition of a selection of tri block co polymers at varying concentrations to the above mentioned surfactant mixture of SDS and OA could influence the particle size. The Pluronics are represented as a percentage weight of the total volume due to their non-specific molecular masses, and the discussion focuses on their influence on the surfactant SDS/OA system with all other reagents constant. The detailed series of reaction data is outlined in Table 2 with related TEM images shown in Figure 1, 2. As the primary trial, Pluronic P123 was mixed in the SDS/OA system at a concentration of 0.15% (R_2). The particles obtained in this experiment were measured to be ~30 nm (Figure 1A, B) with insignificant change of their size as compared to the particles generated in SDS/OA system (R_1). With an increase of concentration of P123 to 0.3% (R_3) in the similar system, a large number of reduced sized particles (~11 nm) were

formed with a smaller number density of ~34 nm particles (Figure 1C). The smaller particles of R_3 can be separated very easily by centrifugation (Figure 1D) revealing the average size to be 11 ±1.3 nm, (inset) by a particle size distribution analysis. With the anticipation of further size reduction, the P123 concentration was increased to 3% (R_4) which is greater than its critical micellar concentration (CMC) [41,42]. Here we could find a host of 30 nm particles along with the presence of light shaded spherical area typical of the structure of block copolymer micelles after drying on a grid [43], Figure 1E. A higher magnification image revealed the presence of very small particles (~ 3-4 nm) localised onto the surface of one such spherical tri block copolymer-micelle, Figure 1F. The image is very much similar to Au nanoparticles encapsulated in a block copolymer sheath reported by Bae et al [36]. Very interestingly, at this concentration of P123, the system could be stabilized even in the absence of SDS. The TEM images (Figure 2A, B) and particle size distribution analysis (Figure 2C) evidenced highly monodispersed 3.7 ± 0.52 nm Ni particles formed only with 3% P123 combined with OA (R_5). The presence of face centred Ni (111) plane with d=2.05Å was confirmed from a higher magnification image, inset Figure 2B. Further increasing the concentration of P123 to 5% in the absence of SDS (R_6), results in no appreciable change in particle formation with average particle size of 3.4±0.43 nm confined within a micelle, Figure 2D-F. The constant OA concentration in all experiments was found to be necessary for particle stabilization with typically no particle formation occurring in its absence: a detailed discussion of the effect of changing the OA concentration is included in the Supporting information S2.

It is clear that the effect of the triblock-copolymer is concentration dependent and the discovery that a surfactant concentration of PI23 (3%) can stabilise sub 5 nm particles in the presence of OA is an important synthetic protocol. The affect of PI23 addition in the presence of SDS is expected to be more complex due to the individual micelle forming ability of both these surfactants. While concentrations of P123 < 3% are insufficient to form individual triblock micelles [41,42] there is a clearly a progressive interference with the SDS micelles from 0.15% P123 (R_2) to 0.3% (R_3). The latter triblock concentration most likely generates a polymer-SDS complex, previously observed by Hecht *et al.* [44]. This complex could readily account for the selective particle size reduction to ~11 nm when the bulky polymer-SDS adsorbs on top of the OA capped Ni nanoparticles preventing further aggregation. However, the complex formation at this concentration is only partial with the presence of ~34 nm Ni stabilized with only SDS micelles [23]. Interestingly, a reaction mixture containing only 0.3% P123 and OA without SDS (R_7, Table 2) could only generate 100 nm particles (Supporting information Figure S3A) confirming that the presence of SDS was vital at 0.3% concentration of P123 for stabilization of ~11 nm Ni nanoparticles. However, at this stage if the SDS concentration is increased to 4×10^{-2}M (R_8, Table 2), the system again becomes rich in SDS, diminishing the effect of P123, generating ~25-30 nm particles (Supporting information Figure S3B). At the higher concentration 3% P123 in presence of SDS/OA, P123 alone can form stable spherical micelles in preference to complexing with SDS. Hence both SDS and P123 micelles are present individually stabilizing nanoparticles leading to the formation of both ~34 nm and ~3-4 nm particles (R_4). The occurrence of only ~3.7 nm particles on elimination of SDS (R_5) with 3% P123 and the absence of any further change in particle size beyond 3% P123 (R_6) suggests that the formation of triblock copolymer micelles is critical to particle stabilisation and when formed are more effective than SDS at impeding particle growth.

The successful size reduction of Ni nanoparticles using only 3% P123 in the presence of OA prompted the extension to a range of triblocks with different chain lengths, Figure 3. Among the chosen tri block copolymers, P65 and P85 are more hydrophobic whereas F127 and F88 are more hydrophilic as seen from the relative percentage of PPO and PEO blocks, Table 1. 3% P65 and 3% P85 both can produce sub 5 nm particles as shown in Figure 3A and 3B respectively. P85 generates more polydisperse Ni nanoparticles as compared to P65 even though both of them have comparable percentage of PPO block. Mixing any one of these hydrophobic tri block copolymers (e.g. P65) with P123 did not generate any new features but only sub 5 nm particles in TEM analysis, Figure 3C. The block co-polymers with relatively higher percentage of PEO groups behave entirely differently. Ni

nanoparticles synthesized in 3% F127 mixture were found to have an irregular morphology as compared to R_5 (Figure 3D) with several crack propogations clearly visible from the magnified image, inset Figure 3D. Moreover the size of particles (~80-100 nm) suggests that F127 is not effective to stabilize sub-5 nm Ni. The poor crystalline nature of these particles is quite evident from its XRD curve, inset of Figure 3D. But the presence of a peak at 44.5^{O} indicates the particles are fcc Ni. The aggregated nature of the Ni particles is also very pronounced in 3% F88, Figure 3E. A mixture of 3% P123/F127 showed the presence of particles typical of those obtained from their individual combinations (Figure 3F). Basically in a mixed block copolymer system, the polymers retain their own micelle formation characteristics and control the size of the Ni nanoparticles accordingly. This study confirmed that more hydrophobic block co-polymers (higher % of PPO) e.g P123 are the more effective to stabilize OA capped Ni nanoparticles resulting in a reduced size range whereas the least hydrophobic Pluronic F88 are ineffective capping agents forming aggregated Ni.

FTIR analysis of aqueous P123 solutions allowed the onset of micelle formation to be predicted. Figure 4A shows FTIR curves of pure P123 (curve 1), 0.3% P123 solution (curve 2), 3% P123 (curve 3) and 5% P123 (curve 4) respectively. The assignment of vibrational bands for pure P123 is tabulated in Supporting information S4 [45-47]. Spectral features showed significant difference in the region ~900-1400 cm^{-1} when the concentration of P123 was varied. Bands at 963, 1014, 1061, 1150 and 1342 cm^{-1} which can be attributed to vibrational modes in pure polymer, disappeared at the 0.3% concentration of P123 in solution (Curve 2). Moreover, FTIR bands at 1237, 1281, 1298, 1373, 2865 cm^{-1} were broadened considerably in Curve 2 as compared to pure P123 (Curve 1). The vibrational multiplate structure of the pure solid phase collapsed leading to a conformational change when they are dissolved in water particularly as monomers, which is already well known [45-47]. The bands at 963, 1061, 1150 and 1342 cm^{-1} have their weak signature in 3% and 5% P123 solution FTIR profiles (Curve 3 and Curve 4 respectively) which were completely absent in 0.3% P123 solution (Curve 2). Furthermore in Curve 3 and 4, the peaks at 1237, 1281, 1298, 1373, 2865 cm^{-1} are relatively sharp as compared to Curve 2. Both these observations suggest a microenvironment change at higher concentration most likely due to micellization. Analogous FTIR signals for 3% (Curve 3) and 5% (Curve 4) P123 solution further suggest the micellar structure remains similar at these two different concentrations. The evidence of a micro-environment change when the concentration of P123 was varied from 0.3% to 5% helped to hypothesize the mechanism of stabilization of Ni nanoparticles in the presence of tri block copolymers.

The FTIR signals obtained from Ni nanoparticles synthesized only with SDS/OA (R_1) and Ni nanoparticles from R_3 (having additional 0.3% P123), R_5 (3% P123) and R_6 (5% P123) are outlined in Curves 1-4 in Figure 4B. Pure OA has its strong –C=O stretching band for carboxylic group at ~1707 cm^{-1} (Supporting information S5A) which is generally shifted to lower wavenumber due to complexation [48-50]. In Curve 1, where the Ni nanoparticles are expected to be capped by the carboxylic acid group of OA, a peak at ~1559 cm^{-1} was observed which can be attributed to bound carboxylate, since pure OA or SDS has no peak at that wavenumber (Supporting information S5A and S5B).The peak prevailed for R_3 in Curve 2. But the appearance of 1103 cm^{-1} peak is due to C-O-C stretching from Pluronic P123 confirming the presence of P123 along with bound OA and SDS on the surface of Ni nanoparticles of R_3. The FTIR curves of R_5 and R_6 are more like P123 apart from the fact that the signature of bound OA is retained at ~1579 cm^{-1}. As the concentration of OA used for the synthesis is low as compared to SDS or P123 the band of –C=O stretching signal is relatively weak and the region of 1450-1750 cm^{-1} is magnified in Figure 4C which presents the bands more clearly.

It can be postulated from the FTIR analysis that P123 forms a similar micellar structure at 3% and 5% concentration and is thus able to stabilize nanoparticles of similar size (3.4-3.7 nm). Also, OA is the capping agent for the Ni nanoparticles in all the samples and it interacts with the nanoparticle surface directly through its polar –COOH group with resultant protrusion of its hydrocarbon chain rendering the Ni particles hydrophobic [5]. This factor is responsible for their stabilization into the hydrophobic core of the tri block copolymer. The hydrophobic PPO chain was able to restrict the growth of Ni particles efficiently and a better size selection is observed at higher concentration of

P123. This hypothesis of stabilization of Ni nanoparticles within the P123 micelles is schematically shown in Figure 5. Here the hydrophobic core is shown to accommodate OA capped Ni nanoparticles and the PEO corona forms a hydrophilic envelop surrounding a group of particles which are embedded into the core making the whole system thoroughly water-dispersible. Similar possibility of stabilization of nanoparticles inside the hydrophobic core is also reported by Jain *et al.*[5] and Chen *et al.* [35] This scheme is applicable when the concentration of P123 is higher than its CMC (≥ 3%).

Figure 6 and 7 represents the routine characterization of XRD and XPS measurements for ~11 nm Ni from R_3 and ~3.7 nm Ni of R_5. X-ray diffractograms of the as prepared samples [Curve 1 for R_3 and Curve 2 for R_5] showed the presence of certain amount of $Ni(OH)_2$ (Figure 6A) probably due to air drying of the water-based Ni nanoparticles. The peaks were extremely broad and the most intense (111) peak at $2\theta=44.6^o$ can be fitted with the components for both metallic fcc Ni and $Ni(OH)_2$. The estimated size of the Ni nanoparticles obtained from these peaks using Scherrer formula is ~14 nm and 1.2 nm for R_3 and R_5 respectively. The particle size of R_3 matches well with TEM analysis, but that of R_5 was lower than TEM results. The discrepancy with the smaller particles may arise due to multi component fitting of the selected peak. The formation of hydroxides was avoided by immediately heating the pellet after centrifugation in an inert atmosphere (N_2) at 250 ^oC for 30 min, (Figure 6B). The XRD peaks in Figure 6B can be indexed to pure fcc Ni for both the samples (PCPDF file no. 04-0850). The size of the heated Ni particles of R_3 and R_5 were found to be ~17 nm and ~8 nm respectively, as estimated from Scherrer analysis. There is no significant change in the size of R_3 but the size of R_5 here is found to be almost doubled. A TEM image of R_5 on the similarly heated sample revealed that the particles are mainly discrete in nature having an average particle size of ~4 nm with some coalescence (Supporting Information S6). The heating under N_2 atmosphere at an elevated temperature improves the crystallinity of the sample without significant sintering.

Figure 7A-C shows the XPS analysis of C1s, O1s and Ni2p levels of ~11 nm Ni nanoparticles of R_3 whereas Figure 7D-F are the similar spectral analysis of ~3.7 nm Ni from R_5. In both the cases C1s peak can be resolved into three components at 284.8, 284.2 and 288.6 eV, Figure 7A and 7D. The two higher binding energy components are probably due to carbon bonded to oxygen e.g. Pluronics ether linkage (C-O-C) and oleic acid (-COOH) respectively. O1s peak can be fitted with single symmetric component for both the samples (Figure 7B and 7E). Similar curve fitting for C1s and O1s for R_3 and R_5 indicates similar ligand environment on the surface of the Ni nanoparticles apart from the fact that S2p signals can be observed for R_3 (Supporting information S7). This agrees with the expectation as R_3 contains SDS was along with Pluronics whereas R_5 does not. The S2p peak can be deconvoluted into two peaks at 168.7 and 170 eV binding energy definitely arising from $S2p_{3/2}$ and $S2p_{1/2}$ levels of $-SO_4$ group of SDS. The XPS signature of Ni2p and its satellite for both R_3 and R_5 (Figure 7C and 7F) are present in the region 845-870 eV. Detailed analysis at this region showed the presence of two main peaks at 852 eV and 855 eV. The higher binding energy peak could be assigned to $Ni(OH)_2$/NiO species. Since the Ni nanoparticles heated under N_2 did not show the presence of $Ni(OH)_2$/NiO species, the XPS results indicate the possibility of adsorbed Ni^{2+}(oleate) complex on the surface of these nanoparticles. The similar results in XPS analysis were also observed by Couto *et al.* [51] and also by Zanchet and co-workers [52] for colloidal Ni synthesized via completely different routes. It is also interesting to note that there is an distinct increase in the Ni^{2+}(oleate) complex species at 855 eV in Ni nanoparticles of R_5 (3.7 nm). As the particle size goes down there is an increase in the surface area which further enhances the probability of more adsorbed Ni^{2+}(oleate) complex which is reflected in the XPS spectra (R_5, Figure 7F).

The temperature dependence of the magnetic susceptibility for the ~11 nm Ni particles of R_3 and ~3.7 nm Ni of R_5 are shown in Figure 8A and 8B respectively. In all the cases, the applied magnetic field was 10 Oe and the temperature was varied between room temperature (300K) and 3K. Curve 1 in Figure 8A corresponds to the magnetization vs. temperature plot for the R_3 in the zero-field-cooled (ZFC) mode while Curve 2 is the measurement carried out in the field-cooled (FC) mode. Similarly, Curve 1 and Curve 2 in Figure 8B correspond to ZFC and FC magnetization respectively

for ~3.7 nm Ni nanoparticles of R_5. As can be clearly seen, the curves of temperature dependent ZFC and FC susceptibilities are typical of magnetic nanoparticles. Magnetic particles below a certain size regime behave as superparamagnetic particles. The main features characteristic of superparamagnetic particles are: i) the zero-field-cooled, measured using very low magnetic fields, displays a maximum in the susceptibility at a certain temperature, called the blocking temperature, T_B; ii) a divergence in the ZFC and FC susceptibility curves below the blocking temperature and iii) appearance of magnetic hysteresis loop and remnant magnetization below T_B whereas the magnetic hysteresis behaviour disappears above T_B [53].

It is interesting to note that both R_3 and R_5 show two maxima in the ZFC curves. While superparamagnetic particles are fast relaxing and the minimum radii for particle stability over a 1 year period under ideal conditions can be calculated for a material using the equation $r_o^{1yr} \approx (10k_BT/K_u)^{1/3}$ where r_o^{1yr} is the superparamagnetic radii for stability, k_B is Boltzmann's constant, T is the temperature and K_u is the particle anisotropy, the parameters are in SI units [54]. Assuming the anisotropy of bulk Ni [53] and a temperature of 300K then the critical particle diameter for stability over 1 year is ~19 nm. This shows that the ~11 nm particles in R_3 will be entirely stable over the temperature range of interest. For uniaxial particles the blocking temperature is actually related to the size of the magnetic particles and the uniaxial anisotropy constant (K) by the equation: $K = 25k_BT_B/V$ where k_B and V are the Boltzmann constant and the volume of a single particle, respectively, T_B is the blocking temperature. For spherical particles with cubic anisotropy the energy barrier is $\frac{1}{12}$ KV when K is negative with a <111> easy direction as in the case of bulk Ni [55]. This would lead to a modification of the equation from the form $K=25k_BT_B/V$ to the form $K=300k_BT_B/V$, however Ni nanoparticles will typically have uniaxial anisotropy as opposed to a cubic anisotropy. This is attributed to the fact that nanoparticles have a relatively large surface to volume ratio; hence their resultant anisotropy has contributions from surface, stress, shape, magnetocrystalline anisotropic components. The ~11 nm Ni of R_3 shows the maximum at 295K from where FC and ZFC curves diverge, Figure 8A. Considering T_B=295K for this ~11 nm particle and substituting the values into the equation $K = 25k_BT_B/V$ we deduce K to be $1.46X10^6$ erg cm^{-3}. Similar calculation on ~3.7 nm Ni nanoparticles of R_5 where T_B=54K (FC-ZFC divergence point, Figure 7B), the anisotropic constant is deduced as $K=7.03X10^6$ erg cm^{-3}. The calculated value of the anisotropy constant of both the samples is one order of magnitude higher than that of bulk nickel ($0.5x10^5$ erg cm^{-3}) [53]. This increase in the anisotropy constant with a decrease in the size of the magnetic nanoparticles has been previously reported [56] and is attributed to the fact that reduction in the volume of the particle leads to an increase in surface effects. Surface anisotropy is caused by the breaking of the crystal's symmetry at the boundaries of the particles and in general surface anisotropy makes the core of the particle appear to be magnetically softer than the surface. For spherical particles surface anisotropy should average to zero however this is known not to hold true for a nanometre sized particle of a few atomic layers and is the likely reason for the discrepancy between the two anisotropy values reported here and that of bulk [56]. Ni nanoparticles of both R_3 and R_5 show a second maxima at ~22K which may arise due to the magnetic transition of small amounts of $Ni(OH)_2$ [57] since all the magnetic measurements were carried out on as-synthesized air dried samples. The shift in the T_B towards the lower value (from 295K to 54K) due to reduction in size is in good agreement with the reported results [58].

The field dependent magnetic behaviour data of R_3 and R_5 are presented in Figure 8C and 8D respectively. The M–H curves measured at 300 K (well above the blocking temperature) show no hysteresis but at 10 K (below T_B) both the samples have magnetic hysteresis with a coercivity of 600 Oe and 2000 Oe respectively and remnant magnetization which are in accordance with those expected for superparamagnetic particles. At 10K the estimated saturation magnetization of the samples with particle size ~11 nm (R_3) and ~3.7 nm (R_5) were estimated as ~30 and ~17 emu/g respectively. This result is consistent with previous reports in which saturation magnetization increases with particle size increasing. The phenomenon is attributed to high surface/volume ratio and corresponding surface effects (spin canting) [58, 59]. Even at applied fields of 20000 Oe both of the samples demonstrated an

upward trend in their magnetization values with magnetic field applied. This effect could be attributed to the presence of the $Ni(OH)_2$ which posses antiferromagnetic order below the Neel temperature (~22K). For antiferromagnetic nanoparticles, the uncompensated magnetic spins associated with the surface atoms are not negligible and contribute to the net magnetization [60]. While antiferromagnetic nanoparticles may demonstrate hysteresis below their Neel temperature their magnetisation is very small and unlikely to account for the very large emu/g values measured for the samples when compared to that of bulk Ni (~50emu/g).

4. Conclusion.

In summary, sub 5 nm Ni nanoparticles were synthesized via a facile water based method by successfully utilizing the novel neutral Pluronic triblock copolymers and oleic acids as stabilizing agents. The magnetic measurements confirm that the Ni nanoparticles are superparamagnetic, a property that can be exploited for example in therapeutic heating or for directing these particles to definite tissues with the help of external magnetic field. The XRD analysis has also shown that although there may be small amount of $Ni(OH)_2$ in the air dried samples, the hydroxide formation can be avoided by drying the samples under inert atmosphere to obtain pure highly crystalline fcc Ni nanoparticles. In addition, the particles thus obtained can be preserved in solution and can also be converted into powder by mere drying without affecting their size which is highly attractive for large scale application e.g. catalytic growth of CNTs. As the reports on the synthesis of sub 5 nm magnetic metallic nanoparticles in a water medium are rare, the facile synthesis of Ni nanoparticles described here using triblock copolymers as a capping agent is an important advance. Neutral surface encapsulation as provided by the Pluronics are highly sought for in-vivo studies of nanoparticles as they have a much extended blood circulation, whereas their sub 5 nm size may allow penetration of tissues with narrow pore cut-off sizes [61].

Acknowledgement.

The work was principally supported by Science Foundation Ireland (SFI) under the Principal Investigator Programme Contract No. 06/IN.1/I85 at UL and by additional funding from SFI PI Grant No. SFI-PI-06/IN.1/I98 at Tyndall, UCC for some of the magnetic measurements. Institutional funding from INSPIRE, the Irish Government's Programme for Research in Third Level Institutions, Cycle 4, National Development Plan 2007-2013 is further acknowledged. Dr. Fathima Laffir is gratefully acknowledged for the XPS analysis of the samples.

Supporting Information.

Basic characterizations (TEM, XRD) of Ni nanoparticles synthesized in SDS/OA mixture (R_1), role of oleic acid on the basis of our experimental results, TEM images of Ni nanoparticles of R_7 and R_8, table containing the designations of FTIR peaks of pure Pluronic P123, FTIR spectra of pure oleic acid and pure SDS, TEM image of heated Ni nanoparticles of R_5 and XPS spectra of S2p level obtained from Ni nanoparticles of R_3 are presented as supporting information. This material is available free of charge via the journal website.

References.

[1] Speliotis D E 1999 *J. Magn. Magn. Mater.* **193** 29.

[2] Gomes J A, Sousa M H, Tourinho F A, Aquino, R, Da Silva G J, Depeyrot J, Dubois E and Perzynski R 2008 *J. Phys. Chem. C* **112** 6220.

[3] Huh Y M, Jun Y W, Song H T, Kim S, Choi J S, Lee J H, Yoon S, Kim K S, Shin J S, Suh, J S and Cheon J 2005 *J. Am. Chem. Soc.* **127** 12387.

[4] Chan D C F, Kirpotin D B and Bunn P A 1993 *J. Magn. Magn. Mater.* **122** 374.

[5] Jain T K, Morales M A, Sahoo S K, Leslie-Pelecky D L and Labhasetwar V 2005 *Molecular Pharmaceutics* **2** 194.

[6] Won J, Kim M, Yi Y W, Kim Y H, Jung N and Kim T K 2005 *Science* **309** 121.

[7] Herr J K, Smith J E, Medley C D, Shangguan D and Tan W 2006 *Anal. Chem.* **78** 2918.
[8] Hiergeist R, Andra W, Buske N, Hergt R, Hilger I, Richter U and Kaiser W 1999 *J. Magn. Magn. Mater.* **201** 420.
[9] Hyeon T 2003 *Chem.Commun*. 927.
[10] Li X K, Ji W J, Zhao J, Wang S J and Au C T 2005 *J. Catal.* **236** 181.
[11] Heracleous E, Lee A F, Wilson K and Lemonidou A A 2005 *J. Catal.* **231** 159.
[12] Fatsikostas A N and Verykios X E 2004 *J. Catal.* **225** 439.
[13] Molina A I, Robles J M, Garcia P B, Castellan E R, Finoechio E, Busca G, Torres P M and Lopez A J 2004 *J. Catal.* **225** 479.
[14] Li Y, Zhang B, Xie X, Liu J, Xu Y and Shen W 2006 *J. Catal.* **238** 412.
[15] Lee K B, Park S and Mirkin C A 2004 *Angew. Chem., Int. Ed*. **43** 3048.
[16] Lee I S, Lee N, Park J, Kim B H, Yi Y W, Kim T, Kim T K, Lee I H, Paik S R and Hyeon T 2006 *J. Am. Chem. Soc.* **128** 10658.
[17] Koltypin Y, Katabi G, Prozorov R and Gedanken A 1996 *J. Non-Cryst. Solids* **201** 159.
[18] Wang H, Jiao X and Chen D 2008 *J. Phys. Chem. C* **112** 18793.
[19] Park J, Kang E, Son S U, Park H M, Lee M K, Kim J, Kim K W, Noh H J, Park J H, Bae C J, Park J G and Hyeon T. 2005 *Adv. Mater*. **17** 429
[20] Chen D H and Wu S H 2000 *Chem. Mater.* **12** 1354.
[21] Capek I 2004 *Adv. Colloid Interface Sci.* **110** 49.
[22] Nagy J B 1989*Colloid Surf.* **35** 201
[23] Sidhaye D S, Bala T, Srinath S, Srikanth H, Poddar P, Sastry M and Prasad B L V 2009 *J. Phys. Chem. C* **113** 3426.
[24] Grzelczak M, Perez-Juste J, Rodrıguez-Gonzalez B, Spasova M, Barsukov I, Farle M and Liz-Marzan L M 2008 *Chem. Mater.* **20** 5399.
[25] Wang H, Kou X, Zhang J and Li J 2008 *Bull. Mater. Sci.* **31** 97.
[26] Mornet S, Vasseur S, Grasset F and Duguet E 2004 *J. Mater. Chem.* **14** 2161.
[27] Gleich B and Weizenecker J 2005 *Nature* **435** 1214.
[28] Weitschies W, Ko¨titz R, Bunte T and Trahms L 1997 *Pharm. Pharmacol.Lett.* **7** 1
[29] Neuberger T, Schopf B, Hofmann H, Hofmann M and Rechenberg B V 2005 *J. Magn. Magn. Mater.* **293** 483.
[30] Gao X P, Zhang Y, Chen X, Pan G L, Yan J, Wu F, Yuan H T and Song D Y 2004 *Carbon* **42** 47.
[31] Bhaviripudi S, Reina A, Qi J, Kong J and Belcher A M 2006 *Nanotechnology* **17** 5080.
[32] Kidwai M, Mishra N K, Bansal V, Kumar A and Mozumdar S 2008 *Catal. Commun.* **9** 612
[33] Sakai T and Alexandridis P 2005 *J. Phys. Chem. B* **109** 7766.
[34] Sakai T, and Alexandridis P 2005 *Nanotechnology* **16** S344.
[35] Chen S, Guo C, Hu G-H, Wang J, Ma J-H, Liang X-F, Zheng L and Liu H-Z 2006 *Langmuir* **22** 9704.
[36] Bae K H, Choi S H, Park S Y, Lee Y and Park T G 2006 *Langmuir* **22** 6380.
[37] Niesz K, Grass M and Somorjai G A 2005 *Nano Lett*. **5** 2238.
[38] Lai J-I, Shafi K V P M, Ulman A, Loos K, Lee Y, Vogt T, Lee W-L and Ong N P 2005 *J. Phys. Chem. B* **109** 15.
[39] Mahmood I, Guo C, Xia H, Ma J, Jiang Y and Liu H 2008 *Ind. Eng. Chem. Res.* **47** 6379.
[40] Alexandridis P and Lindman B 2000 *Amphiphilic Block Copolymers- Self Assembly and Applications*, Elsevier Publication.
[41] Su Y-L and Liu H-Z 2003 *Korean J. Chem. Eng*. **20** 343.
[42] Alexandridis P, Holzwarth J F and Hatton T A 1994 *Macromolecules* **27** 2414.
[43] Xiong X Y, Tam K C and Gan L H 2003 *Macromolecules* **36** 9979.
[44] Hecht E and Hoffmann H 1994 *Langmuir* **10** 86
[45] Dissanayaket M A K L and Frech R 1995 *Macromolecules* **28** 5312.
[46] Su Y-L, Wang J and Liu H-Z 2002 *Langmuir* **18** 5370.
[47] Su Y-L, Wang J and Liu H-Z 2002 *J. Colloid Interface Sci.* **251** 417.

[48] Wu N, Fu L, Su M, Aslam M, Wong K C and Dravid V P 2004 *Nano Lett*. **4** 383.
[49] Wang W, Efrima S and Regev O 1998 *Langmuir* **14** 602.
[50] Bala T, Prasad B L V, Sastry M, Kahaly M U and Waghmare U V 2007 *J. Phys. Chem. A* **111** 6183.
[51] Couto G G, Klein J J, Schreiner W H, Mosca D H, de-Oliveira A J A and Zarbin A J G 2007 *J. Colloid Interface Sci.* **311** 461.
[52] Winnischofer H, Rocha T C R, Nunes W C, Socolvsky L M, Knobel M and Zanchet D 2008 *ACS Nano* **2** 1313.
[53] Cullity B D 1972 *Introduction to Magnetic Materials,* Addison-Wesley Publishing, Reading, MA.
[54] O'Handley R C 2000 *Modern Magnetic Materials, Principles and Applications*, Wiley and Sons Publications ISBN 0-471-15566-7.
[55] Cullity B D and Graham C D 2009 *Introduction to Magnetic Materials, Second Edition*, IEEE press, Wiley and Sons Publication, ISBN 978-0-471-47741-9.
[56] Batlle X and Labarta A 2002 *J Phys. D: Appl. Phys.* **35** R15.
[57] Suzuki M, Suzuki I S and Enoki T 2000 *J. Phys.: Condens. Matter*. **12** 1377.
[58] Wang H, Jiao X and Chen D 2008 *J. Phys. Chem. C* **112** 18793.
[59] Ngo A T, Bonville P and Pileni M P 2001 *J. Appl. Phys.* **89** 3370.
[60] Parda C and Moran E 2006 *Chem. Mater.* **18** 2719.
[61] Melancon M P, Lu W and Li C 2009 *Mater. Res. Bull.* **34** 415.

Table 1. Properties of Pluronic tri block co-polymers used in this study

Pluronic	Representative formula	% EO	%PO	PPO/PEO ratio
P123	$(PEO)_{19}(PPO)_{69}(PEO)_{19}$	36	64	1.77
P65	$(PEO)_{20}(PPO)_{30}(PEO)_{20}$	57	43	0.75
P85	$(PEO)_{26}(PPO)_{39}(PEO)_{26}$	57	43	0.75
F127	$(PEO)_{106}(PPO)_{69}(PEO)_{106}$	74	26	0.35
F88	$(PEO)_{102}(PPO)_{39}(PEO)_{102}$	84	16	0.19

Table 2. Concise information on the experiments carried out varying the concentration of SDS and Pluronic P123 for the synthesis of Ni nanoparticles. The concentration of oleic acid and $Ni(NO_3)_2$ was maintained at 10^{-4} M and 10^{-3} M respectively in every reaction varying the concentration of SDS and P123.

Reaction index as mentioned in text	[SDS]	[P123]	Particle size	Image index
R_1	10^{-2} M	0 %	~34 nm.	Sup Info. S1
R_2	10^{-2} M	0.15 %	~30-34 nm.	Fig. 1A-B
R_3	10^{-2} M	0.3 %	Bimodal ~34 and 11 nm.	Fig. 1C
R_4	10^{-2} M	3% (>CMC)	Bimodal ~34 and 3-4 nm.	Fig. 1E-F
R_5	0 M	3% (>CMC)	~3.7 nm particles.	Fig. 2A-B
R_6	0 M	5% (>CMC)	~3.4 nm particles.	Fig. 2D-E
R_7	0 M	0.3 %	~100-200 nm aggregated particles.	Sup Info. S3A
R_8	$4X10^{-2}$ M	0.3 %	~25-30 nm.	Sup Info. S3B

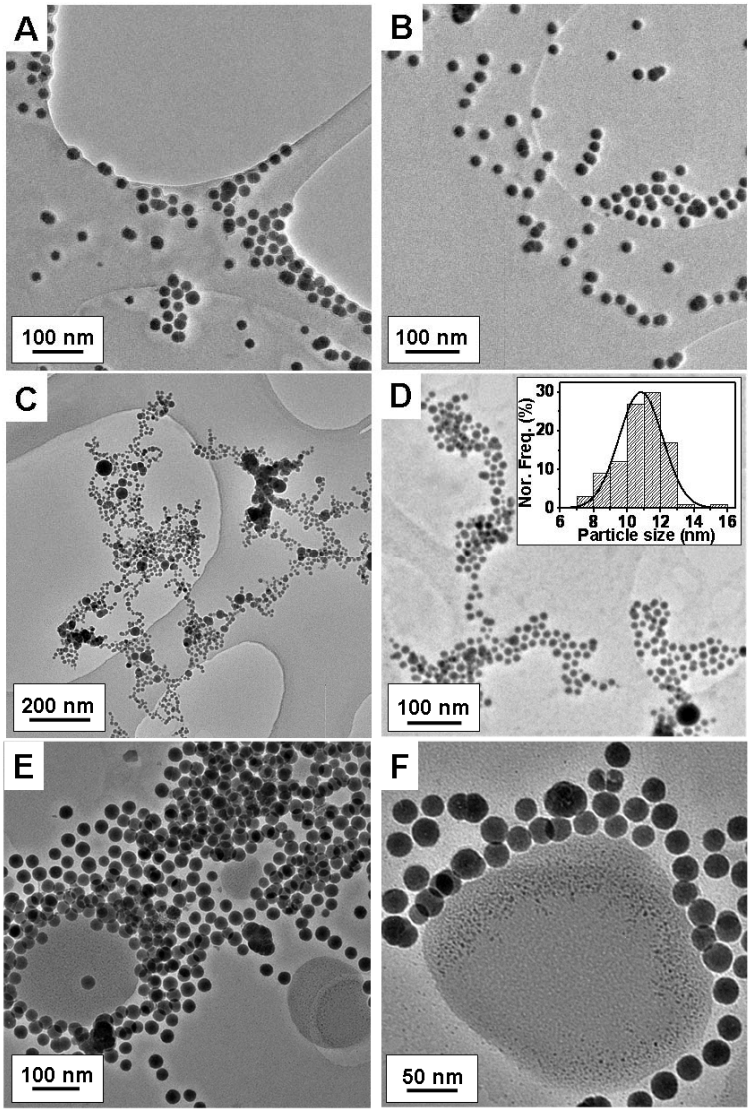

Figure 1. TEM images of Ni nanoparticles formed in presence of SDS/OA/0.15% P123 in R_2 (A, B), SDS/OA/0.3% P123 in R_3 (C, D), SDS/OA/3% P123 in R_4 (E, F). Particle size distributions of R_3 after centrifugal separation of ~11 nm Ni is shown in inset of D.

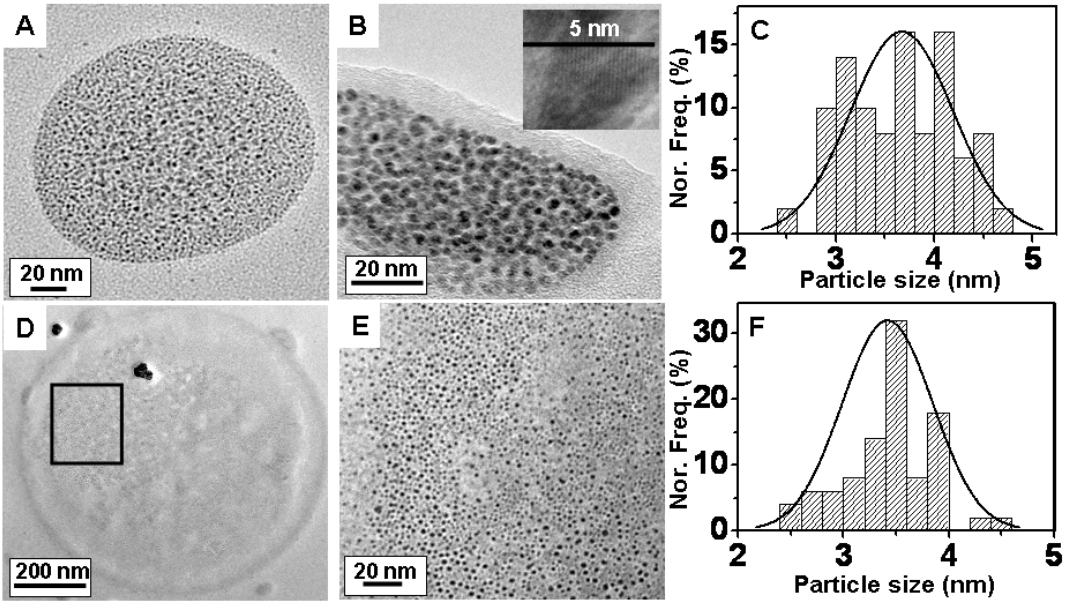

Figure 2. (A, B) TEM images of Ni nanoparticles formed in presence of OA/3% P123 in R_5 (C) Particle size distributions of R_5. (D, E) TEM pictures of Ni produced with OA/5% P123 in R_6. The square marked region in (D) is shown in higher resolution in (E). (F) Particle size distributions of R_6.

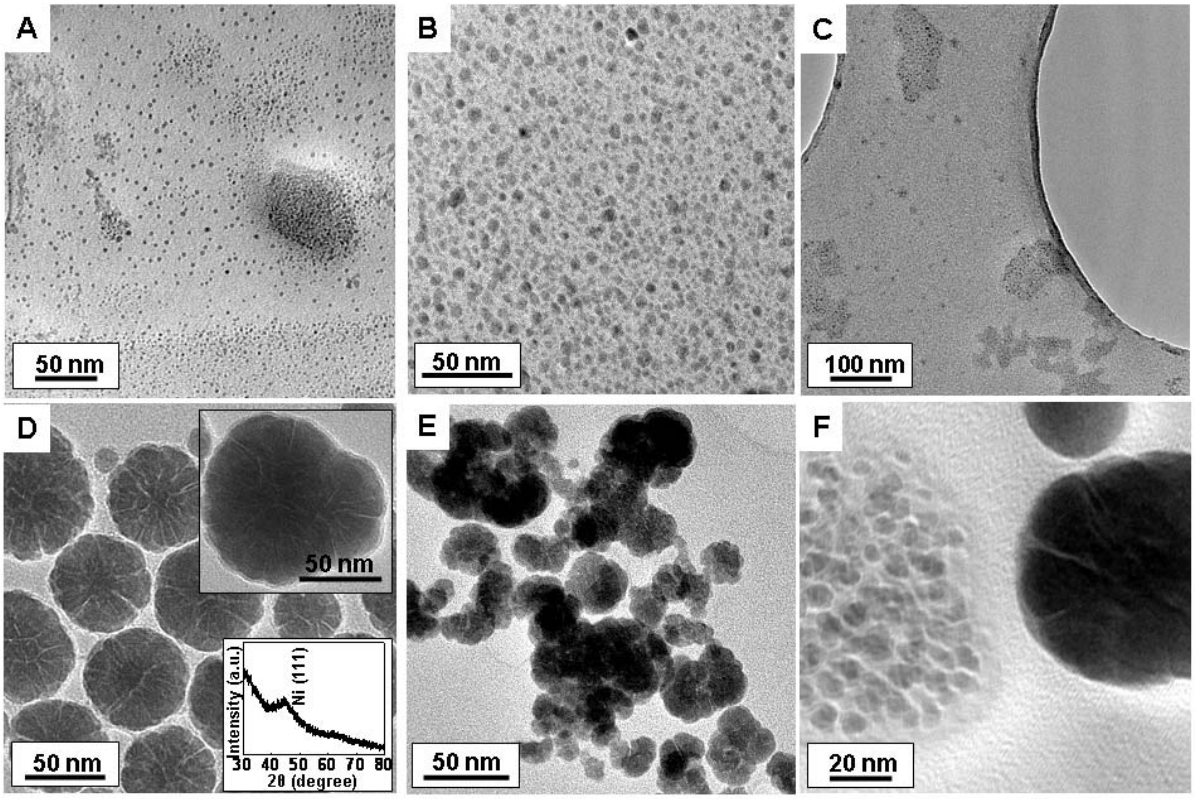

Figure 3. TEM images showing the effect of decreasing hydrophobicity on the nature of the Ni nanoparticles formed with different Pluronic block co-polymers; P65 (A), P85 (B), P65/P123 (C), F127 (D), F88 (E) and F127/P123 (F). The insets of (D) show the magnified image of the structure of Ni formed with 3% F127 and also the X-ray diffractogram of the same sample.

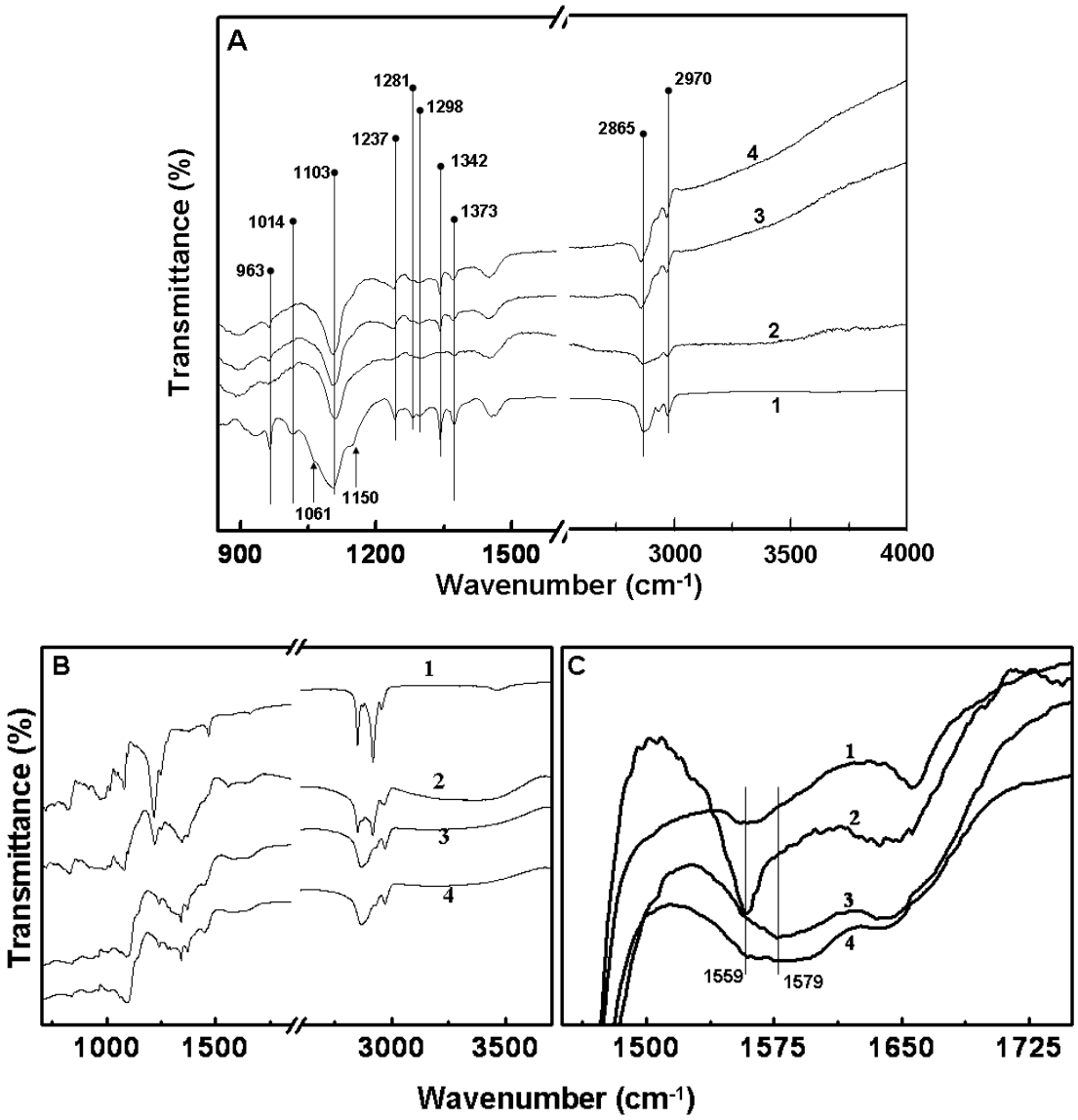

Figure 4. (A) FTIR spectra of pure Pluronic P123 (Curve 1), Aqueous solution of 0.3% P123 (Curve 2), 3% P123 (Curve 3) and 5% P123 (Curve 4). (B) The FTIR spectra obtained from the Ni particles bound to SDS/OA (Curve 1), SDS/OA/0.3% P123 (Curve 2), OA/3% P123 (Curve 3), OA/5% P123 (Curve 4). (C) Highlighting the FTIR spectra of the same samples as mentioned in (B) in the region of 1450-1750 cm^{-1}.

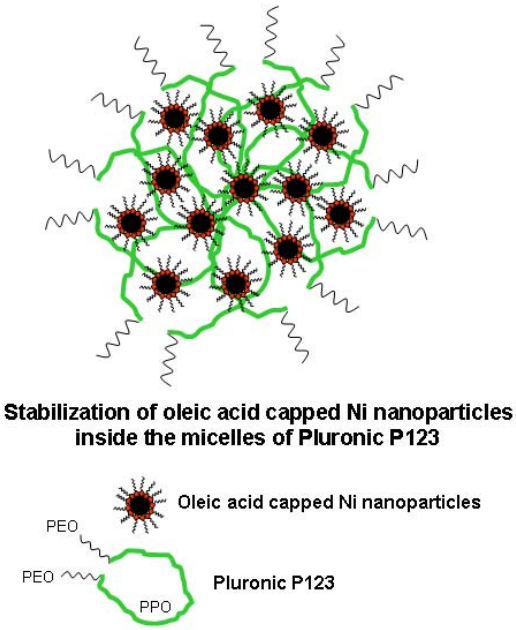

Figure 5. Scheme showing the proposed micellar structure where oleic acid capped Ni nanoparticles are accommodated inside the tri block copolymer micelle.

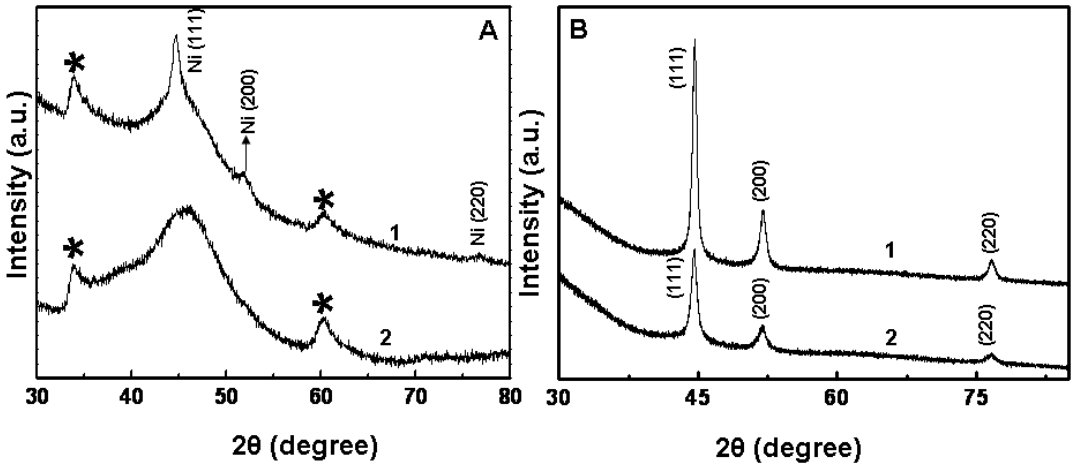

Figure 6. (A) X-ray diffractograms of as prepared Ni nanoparticles from R_3-11nm (Curve 1) and R_5-3.7 nm (Curve 2). The peaks marked with * could be matched with $Ni(OH)_2$. (B) XRD analysis of the samples after heating. Curve 1 corresponds to 11 nm Ni nanoparticles of R_3 and Curve 2 to 3.7 nm Ni nanoparticles of R_5 respectively. The peaks can be indexed for pure fcc Ni.

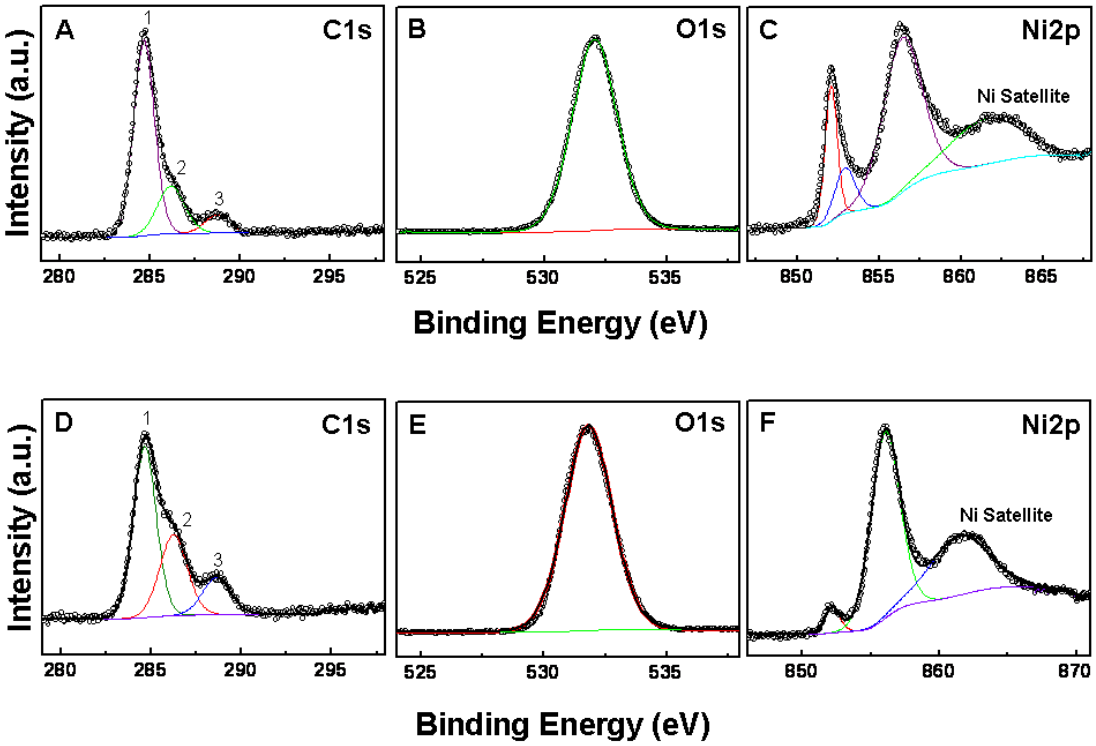

Figure 7. X-ray photo electron spectra of C1s, O1s and Ni2p obtained from 11 nm Ni nanoparticles of R_3 (A-C) and 3.7 nm Ni nanoparticles of R_5 (D-F).

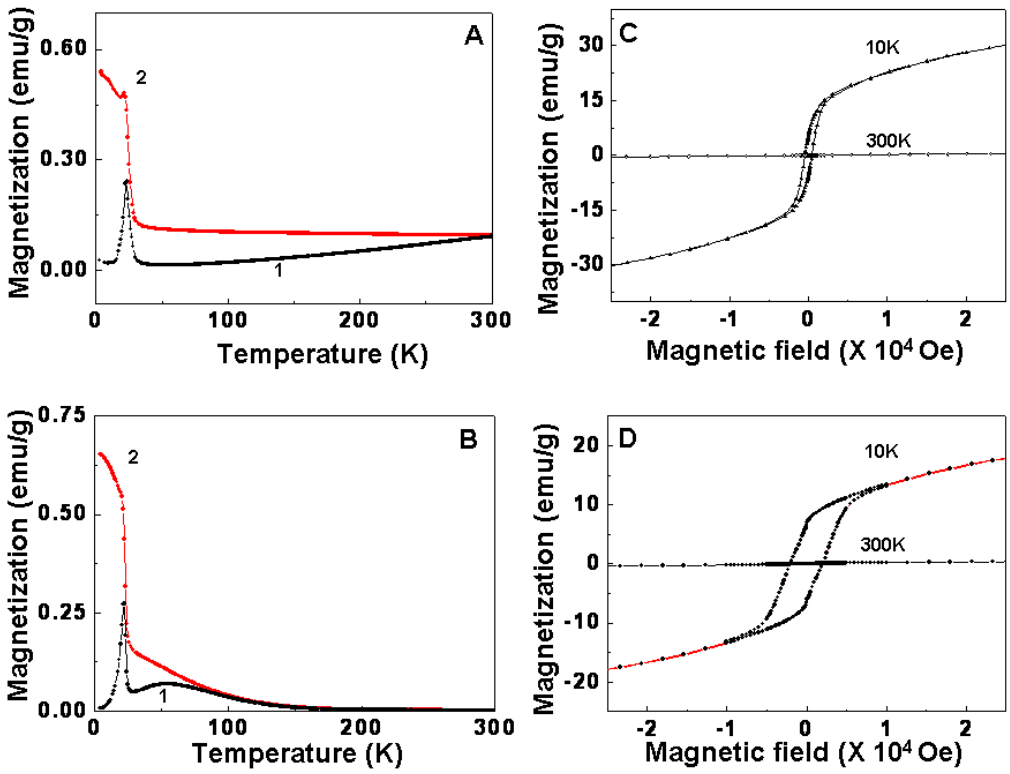

Figure 8. Temperature dependent Zero Field Cooled (Curve 1) and Field Cooled (Curve 2) magnetization curves for 11 nm Ni nanoparticles of R_3 (A) and 3.7 nm Ni nanoparticles of R_5 (B) showing the blocking temperatures of the respective samples. The field dependent magnetization hysteresis loops below (10K) and above (300K) the blocking temperatures of the respective samples are presented in (C) and (D).

Supporting Information

S1

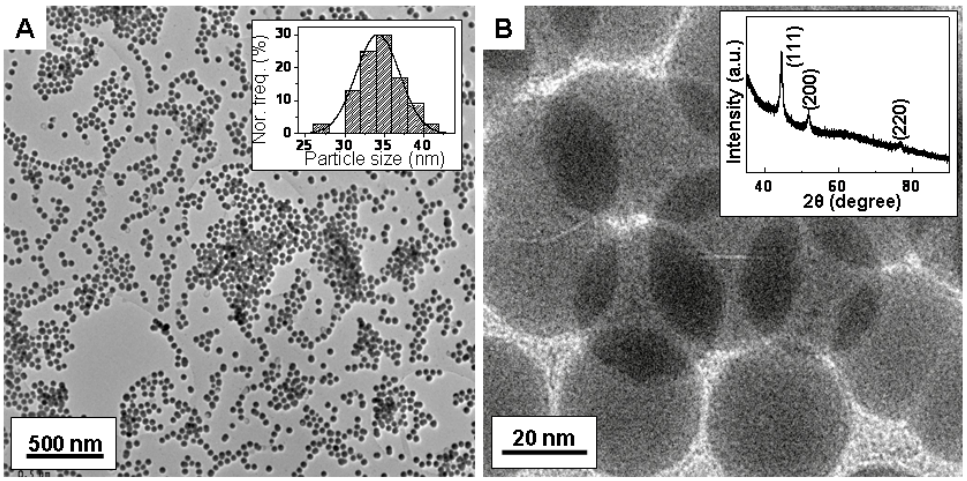

Figure S1. (A, B) Transmission electron micrographs of Ni particles formed with an optimum concentration of SDS and oleic acid following the route reported by Prasad and co-workers [23]. Particle size distribution in the inset of (A) shows the average size as ~34±2.8 nm. XRD characterization shown as inset of (B) can be indexed for fcc Ni confirming the crystalline nature of the particles.

Supporting Information

S2

Role of oleic acid on the basis of our experimental observations:

The OA concentration was constant at 10^{-4} M in all the experiments as its presence is of prime importance along with the other surfactants (e.g. SDS or block copolymers) to stabilize the system. Removal of OA from the surfactant mixture results in no particle formation as observed by a change in the reaction solution from black to colourless within a few hours, probably due to the inherent tendency of Ni^0 state to be converted into Ni^{2+}. In fact oleic acid is already well-known for its capping ability, particularly for various magnetic nanoparticles including Co, Ni, iron oxides or ferrites [S1-S6]. However, carrying out the reaction in the absence of other surfactants and using OA alone results in the generation of bigger particles in the size range of ~80-100 nm [S5]. Thus it can be hypothesized that oleic acid has its prime role to passivate the particles from aerial oxidation but has limited ability to restrict the growth of particle size on its own without the presence of additional capping agents.

[S1] Samia A C S, Hyzer K, Schleuter J A, Qin C-J, Jiang J S, Bader S D and Lin X-M 2005 *J. Am. Chem. Soc.* **127** 4126.

[S2] Bala T, Bhame S D, Joy P A, Prasad B L V and Sastry M 2004 *J. Mater. Chem.* **14** 2941.

[S3] Fried T, Shemer G and Markovich G 2001 *Adv. Mater*. **13** 1158.

[S4] Bala T, Rajsankar C, Baidakova M, Osipov V, Enoki T, Joy P A, Prasad B L V and Sastry M 2005 *Langmuir* **21** 10638.

[S5] Bala T, Joshi B, Iyer N, Sastry M and Prasad B L V 2006 *J. Nanosci. Nanotechnol.* **6** 3736.

[S6] Lee S-Y, Harris M T 2006 *J. Colloid Interface Sci.* **293** 401.

Supporting Information

S3

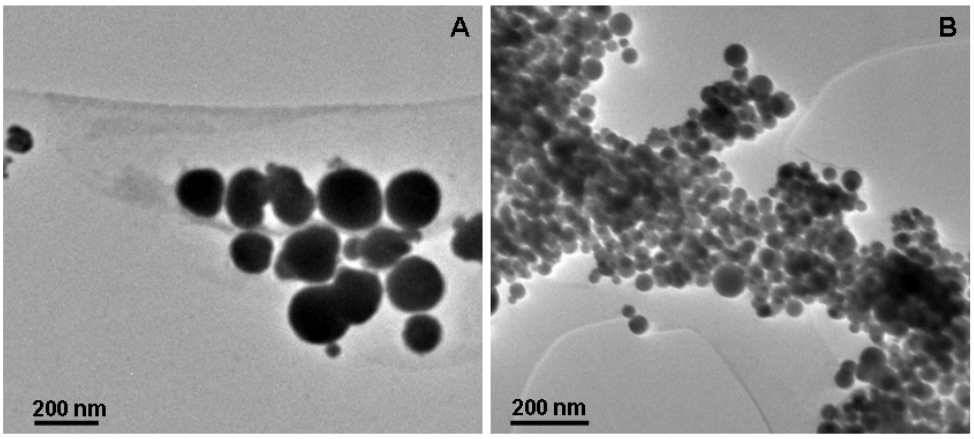

Figure S3. (A) Transmission electron micrographs of Ni particles formed without SDS by combination R_7. (B) TEM showing Ni nanoparticles of average size ~25-30 nm formed in the reaction R_8.

Supporting Information

S4

Table S4. Assignment of FTIR bands of Pluronic P123 according to Ref 45-47.

Peak positions of P123 (cm^{-1})	**Assignment**
963	CH_2 antisymmetric rock
1061 (shoulder)	C-O-C antisymmetric stretch, CH_2 symmetric rock
1103	C-O-C symmetric stretch
1150 (shoulder)	C-C stretching, C-O-C antisymmetric stretch
1237	CH_2 antisymmetric - symmetric twist
1281	CH_2 antisymmetric + symmetric twist
1342	CH_2 antisymmetric wag
1373	Methyl group symmetric deformation
2970	C-H stretching of methyl group

Supporting Information

S5

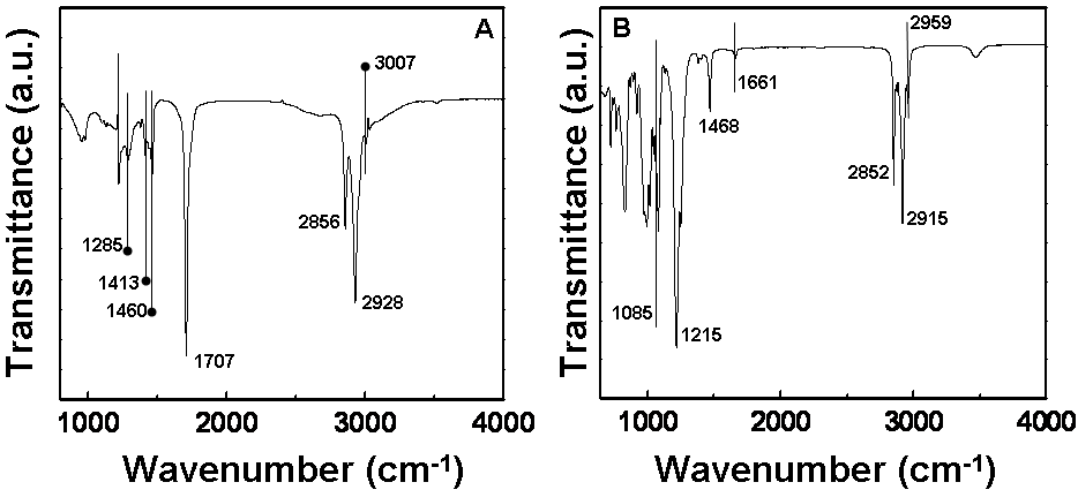

Figure S5. (A) FTIR spectra of pure oleic acid. The 1707 cm^{-1} peak here is attributed to –C=O stretching frequency of free carboxylic acid which is shifted to the lower wavenumber in bound OA. (B) FTIR spectra of sodium dodecyl sulphate (SDS).

Supporting Information

S6

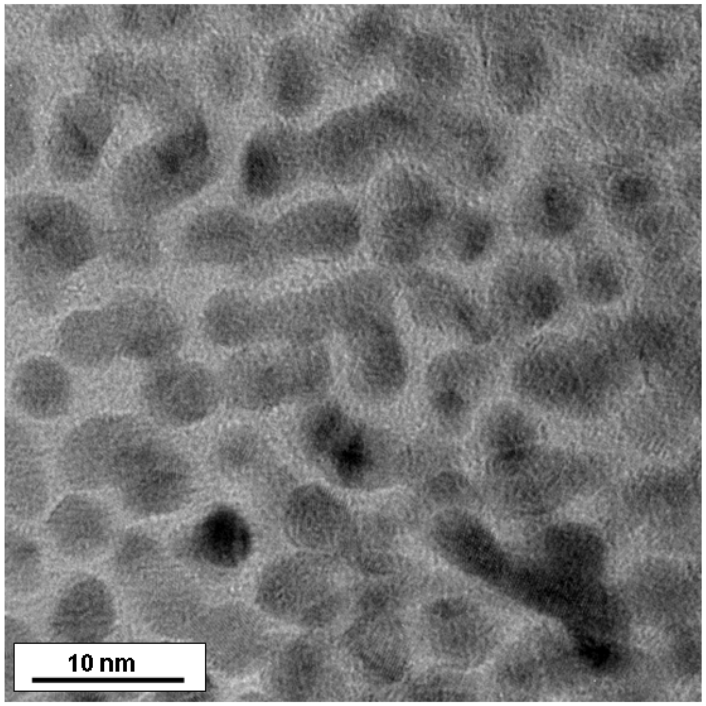

Figure S6. TEM of Ni nanoparticles of R_5 after heating at 250 ^{o}C showing the discrete nature with sub-5 nm particle size.

Supporting Information

S7

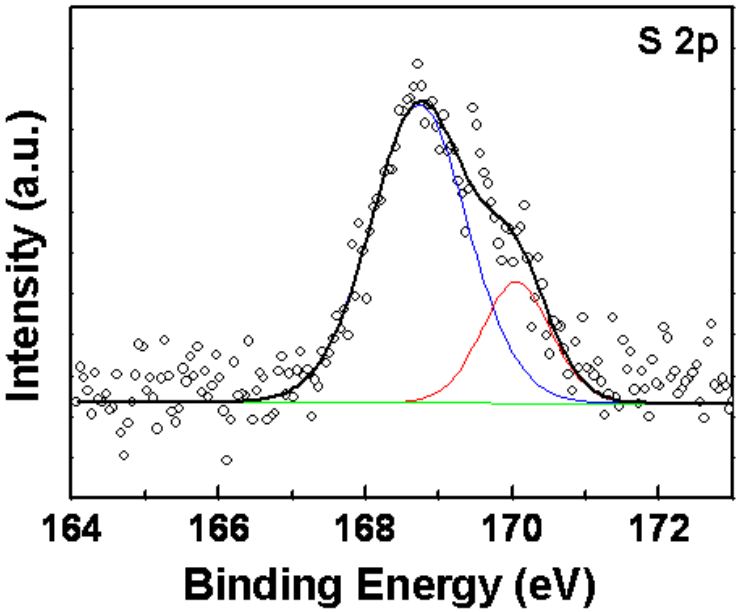

Figure S7. XPS analysis of the S2p level obtained from the Ni nanoparticles of R_3. The presence of $S2p_{3/2}$ peak at 168.7 eV clearly indicates that the signal came from $–SO_4$ group of sodium dodecyl sulphate (SDS).